Numerical Simulation of convection cooling of a turbine blade which examines the amount of heat transfer and the effect of applying different superalloys in the distribution of heat and stress on the turbine blade

Alireza Bakhshinejad Bahmbary [1 *]

[*]Corresponding author: alirezabakhshenegad@gmail.com
[1]*Faculty of Mechanical Engineering, Shahrood University of technology, Shahrood*

Abstract

In this study, by comparing several different superalloys, the stress concentration and heat distribution on the numerically simulated blade with Internal cooling are investigated. The suitable model for examining this simulation is the k-ε turbulence model. The calculation of this simulation was solved by finite element analysis software. By comparing different superalloys and calculating the Stress and the diffused heat generation, we were able to find the alloy with the lowest thermal stress in blades suction and pressure side. Also, according to the results obtained from simulation of the turbine blade, it can be noted that there is a concentration of thermal stress, especially on the leading and trailing edge of blade.

Keywords: Heat Transfer; Thermal stress; Convection Cooling; Temperature distribution; Tension concentration; superalloys; turbine Blade

1. Introduction

The operating temperature of the turbine is much higher than the permitted temperature of the blades, so cooling the blades is a necessity for the proper operation of turbine. There are several key factors affecting the maintenance and the cooling process of a turbine: material of the blade, which shows its mechanical strength relative to the creep and deformation, the thermal properties of the blade alloy, which is responsible for its conductive heat transfer, An external Flow that generates thermal load, and an internal cooling Flow, which is responsible for reduction of the intensity of the external convective heat.

The advancement of technology and metallurgy leads to the strengthening and reinforcement of alloys. On the other hand, the development of gas turbines and increasing the efficiency and thermal efficiency will require an increase in turbine inlet temperature and Pressure ratios, which will increase the disruption rate with the simultaneous increase in turbine blade thermal load. So it is clear that efficiency of a turbine is in correlation with the maximum amount of temperature the turbine blades can tolerate [1-2]. A lot of efforts have been made to solve the problem of super-warming the blades using a cooling method [3-5]. Thermal stress at high temperatures is not negligible because it reduces the life of the blade and leads to fatigue early on [6]. Therefore, examination of the thermal stresses of the blade under the reduction of the thermal gradient in the blade is necessary. Convectional Heat transfer as shown in Fig. 1 is performed by passing cool air from the inner paths of the blade. The heat is transmitted by the conduction through the blades and then transported by convection to the inner airflow of the blade. There are 3 types of heat transfer between the external flow due to the combustion of hot gas and the air that is flowing in the holes embedded in the turbine blade, the structure and material forming the blade plays a key role in heat conduction.

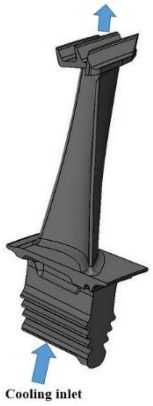

Fig. 1. Convectional Cooling blade

Kyung Min Kim et al. [7] examined the heat transfer coefficient and thermal stress on the blade and obtained the results of the maximum temperature of the

blade at its trailing edge, which is higher than the leading edge of the blade due to the growth of the thermal boundary layer. Candelario Bolaina et al. [8] studied the distribution and propagation of thermodynamic stresses in turbine blades cooled with air flow and the effects of thermal stress concentration on reducing the cooling rate in the blade and the concentration of thermal stress in the leading edge and root of the blade. Daniel Dragomir-Stancia et al. [9] using finite element method and turbine blade simulation in Ansys software, measured the amount of mechanical strength of a blade (with or without a cooling hole with ceramic coating) and proposed a method to reduce the aforementioned tension. Bingxu Wang et al. [10] tried to optimize the shapes, locations and dimensions of the internal cooling passages within a turbine vane to achieve a design that minimizes the average temperature and ensures structural strength within the three kinds of shape configurations: Circular, superellipse and near-surface holes models with different positions in the width of the blade to reduce the temperature without reducing the mechanical strength up to a maximum of 50 k. R.K. Mishra et al. [11] examined the failure of an un-cooled turbine blade which had failed due to malfunction of sensors in the engine control system. This paper proved that the failure had originated from the leading edge and then propagated towards the trailing edge.

In this paper, the extent of the temperature range, the stress and the thermal diffusion in the second row (intermediate pressure section) of a gas turbine which is being cooled internally by the means of convection in three dimensions, will be discussed. Finally an evaluation between different superalloys used in turbine blades, will provide us with a superalloy with a reasonable temperature range and low thermal tension gradient.

2. Solving method

We have used a finite element software to solve this problem and assumed that air is compressible. The domain of our study includes a 3D steady-state turbulent flow and steady-state condition was assumed while calculating thermal stress and temperature range.

2.1 Mathematical equations governing the solution

The governing equations in this Simulation are the conservation of mass, Energy and Momentum. Turbulence equation consists of small eddies that are continuously formed and evacuated. Reynolds stresses are calculated at average speeds. These equations work in accordance with the assumptions made [12].

$$\frac{\partial \rho}{\partial t} + \frac{\partial}{\partial x_j}\left(\rho U_j\right) = 0$$

(1)

$$\frac{\partial \rho U_i}{\partial t} + \frac{\partial}{\partial x_j}\left(\rho U_i U_j\right) = -\frac{\partial p'}{\partial x_i} + \frac{\partial}{\partial x_j}\left[\mu_{eff}\left(\frac{\partial U_i}{\partial x_j} + \frac{\partial U_j}{\partial x_i}\right)\right] + s_M$$

(2)

Where S_m is the sum of the forces implied on the surface and μ_{eff} is the effective viscosity calculated from the following equation.

$$\mu_{eff} = \mu + \mu_t$$

(3)

The value of μ_t for simple eddy models is:

$$\mu_t = \rho f_\mu U_t l_t$$

(4)

f_μ is the 'constant of proportion' and l_t is obtained from the formula below:

$$l_t = \left(V_D^{\frac{1}{3}}\right)/7$$

(5)

μ_t is turbulence viscosity and according to the K-ε model ,it is related to the kinetic energy of turbulence and dissipation and is calculated by the following equation:

$$\mu_t = \rho c_\mu \frac{k^2}{\varepsilon}$$

(6)

And P' is the corrected pressure as defined by the following equation:

$$p' = p + \frac{2}{3}\rho k + \frac{2}{3}\mu_{eff}\frac{\partial U_k}{\partial x_k}$$

(7)

The equation used to calculate the turbulence of this problem is the turbulent flow model K-ε, which is based on the Navier Stokes standard deviation group analysis. In this equation, K calculates the kinetic energy values of turbulence and the amount ε are losses due

to depreciation and rotational flows. The corresponding equation is as follows:

$$\frac{\partial(\rho k)}{\partial t}+\frac{\partial}{\partial x_j}\left(\rho U_j k\right)=\frac{\partial}{\partial x_j}\left[\left(\mu+\frac{\mu_t}{\sigma_k}\right)\frac{\partial \mathrm{k}}{\partial \mathrm{x}_j}\right]+P_K-\rho\varepsilon+P_{Kb} \quad (8)$$

$$\frac{\partial(\rho \varepsilon)}{\partial t}+\frac{\partial}{\partial x_j}\left(\rho U_j k\right)=\frac{\partial}{\partial x_j}\left[\left(\mu+\frac{\mu_t}{\sigma_\varepsilon}\right)\frac{\partial \varepsilon}{\partial \mathrm{x}_j}\right]+\frac{\varepsilon}{k}\left(C_{\varepsilon 1}P_K-C_{\varepsilon 2}\rho\varepsilon+C_{\varepsilon 1}P_{Kb}\right)$$

(9)

The value of P_k in the equation above is calculated from the following equation for turbulent flow:

$$P_K=\mu_t\left(\frac{\partial U_i}{\partial x_j}+\frac{\partial U_j}{\partial x_j}\right)\frac{\partial U_i}{\partial x_j}-\frac{2}{3}\frac{\partial U_k}{\partial x_k}\left(3\mu_t\frac{\partial U_k}{\partial x_k}+P_{Kb}\right) \quad (10)$$

The fixed values in the K-ε equations are given in Table 1:

Table 1. Constants of the equations K-ε

$C_{\varepsilon 1}$	$C_{\varepsilon 2}$	C_μ	σ_k	σ_ε
1.44	1.92	0.09	1	1.3

3. Simulation and numerical solutions

The geometry of the blade is shown in Fig. 2. This blade has an internal air passage for cooling which transmits convectional heat transfer relative to the hot blade body. The blade is constraint to its root and the assumption of non-deformation is considered. The CFX part of this software is used as a solver for heat transfer, pressure and temperature equations.

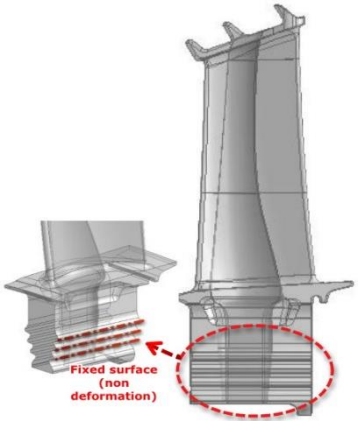

Fig. 2. Blade geometry

First, we define a domain around the blade, according to the requirements of the problem and the facilities in the software, in order to determine the boundary conditions and start meshing. The total number of nodes in the domain is approximately 1.5 million and the total number of Elements is about 1.4 million.

3.1 Expression of the problem and definition of boundary conditions

Before entering the problem solver, we define the boundary conditions for the inlet and outlet conditions of the air as well as the conditions on the walls. At the entrance of this domain, hot air is fed at a pressure of 1.322 MPa and a temperature of 1320 K (1046.85 C), and exits at an outlet pressure of 0.929 MPa. The cool air temperature of the inlet to the cooling passage of blade 780 K (506.85 C) and the flow rate of the air is equal to 0.138 kg/s [13-14]. The total number of blades on the turbine wheel is 86. The rotating speed of the blade is considered at the domain of 15000 rev/min. The domain of the analysis of this software is shown in Fig. 6. High definition residuals were monitored and the convergence residuals of 10^{-5} used for the maximum RMS error.

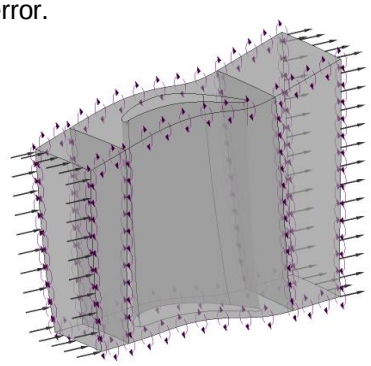

Fig. 3. The domain Modeling for CFD analysis

In section of the heat and Tension analysis, the blade is analyzed using the temperature distribution and temperature range and distribution of stress with using different superalloys. The characteristics of the super alloys used in Fig. 4 and 5 are [15-20].

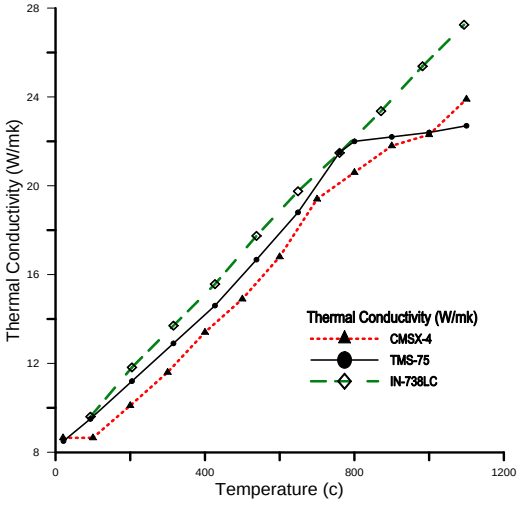

Fig. 4. superalloys thermal conductivity as a function of temperature

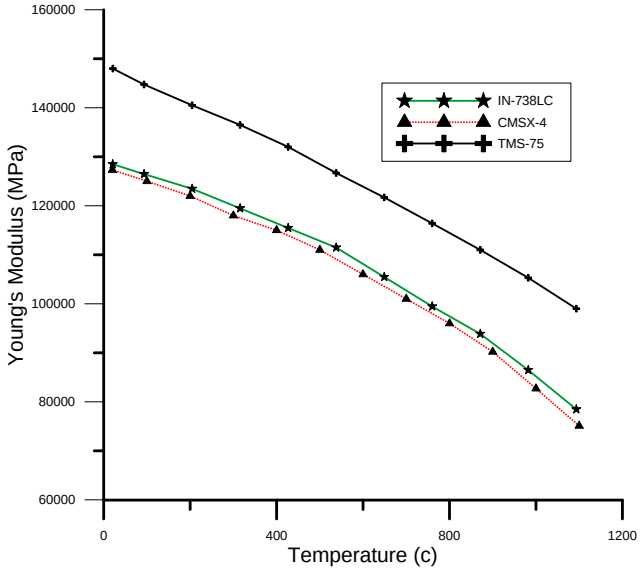

Fig. 5. superalloys Young's modulus as a function of temperature

4. Results

4.1 Flow analysis around the blade

The average heat transfer coefficient at the pressure side of turbine blade and leading Edge where stagnation point is, is higher than the suction side. The growth of the boundary layer increases the heat transfer coefficient at the trailing edge and the walls near the root of the blade, as shown in Fig. 6. Also the heat transfer coefficient of the cooling passage wall is shown in Fig. 7.

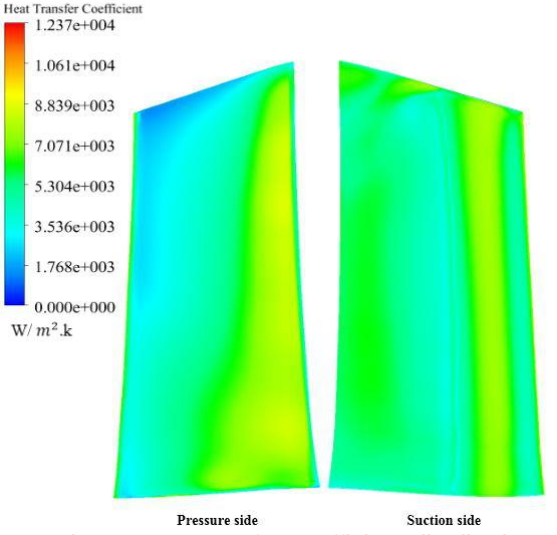

Fig. 6. Heat transfer coefficient distributions on blade surfaces

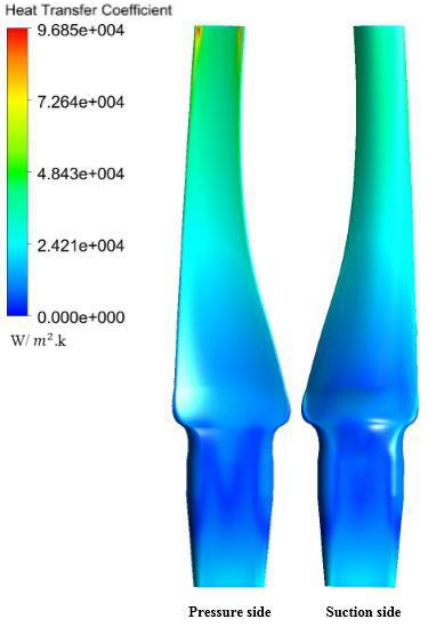

Fig. 7. Heat transfer coefficient distributions on cooling passage of blade

The flow in the collision with the blade at stagnation point is stagnant and the pressure is increased. Flow continues along the path of streamline in the suction side by reducing pressure and increasing speed. As a result of the increase in speed, the Reynolds number of the flow increases, which also increases the Nusselt number, $Nu = 0.023Re^{0.8}Pr^{0.4}$. In Fig. 8 the pressure distribution on suction side of Blade is shown.

To calculate the pressure distribution over the blade height, three sections are used. These three sections show pressure variations in suction and pressure side, as shown in the Fig. 9.

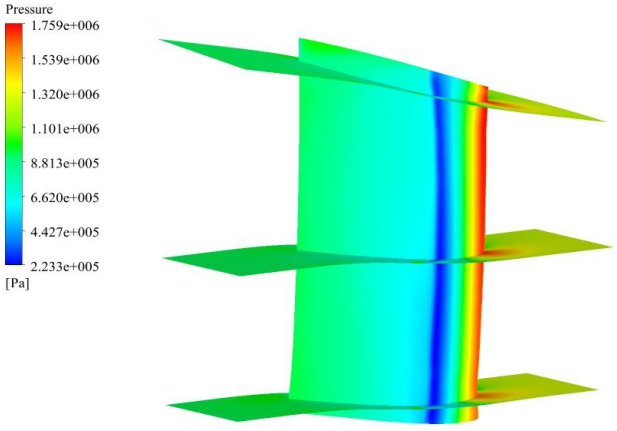

Fig. 8. pressure distribution on suction side of Blade

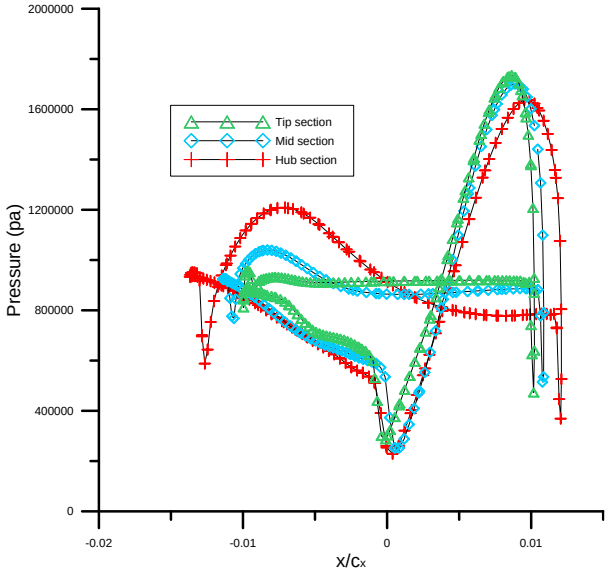

Fig. 9. Pressure variations at different sections

As shown in Fig.9, the high pressure appears at leading edge of the tip section.

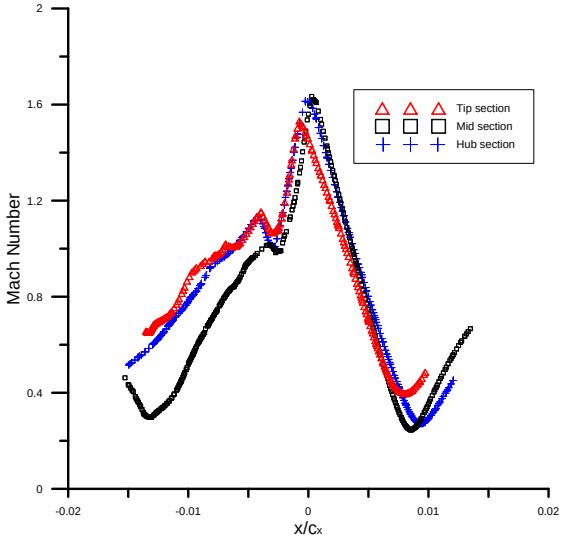

Fig. 10. Mach number at different sections of Blade

The Mach number generated from the inlet condition is shown in the Fig.10 for different sections. The Mid section in leading Edge has the highest Mach number due to the absence of the walls and the absence of the boundary layer.

4.2 Tension and temperature distribution analysis of blade

The highest temperature is at the leading edge at the tip section and at the Trailing Edge of the blade, And due to the increased cross section of the cooling path at each section of the blade, the amount of applied heat in the blade from Tip to Hub has decreased. The Trailing edge of the blade has the highest temperature in each section due to the absence and distancing of the internal cooling passage.

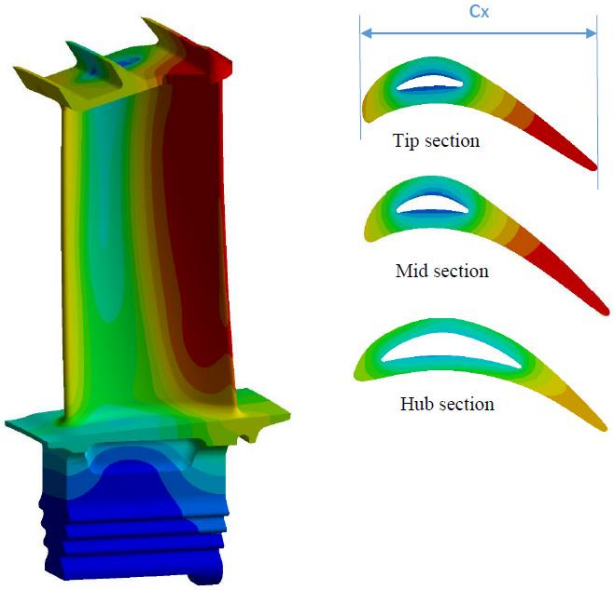

Fig. 11. Temperature distribution at different sections of Blade

The temperature range of the blade, which results from the convectional heat transfer between the two existing air streams with different superalloys, are shown in Table 2.

Table 2. Temperature range of alloys used in blades

Alloys	$T_{min(C)}$	$T_{max(C)}$
CMXS-4	507.37	1102.4
In-738LC	507.5	1101.2
TMS-75	507.43	1102.7

The lowest temperature difference is related to IN-738LC alloy and the highest temperature difference is related to TMS-75 alloy. The IN-738LC alloy, due to its high conduction coefficient, provides a more uniform temperature distribution and a further reduction of the temperature gradient. In the TMS-75 alloy, due to the presence of thermal and ductile resistance properties in the alloy structure, the difference in temperature was higher than that of other alloys, but because of the stability of this alloy particularly at high temperatures and resistance to corrosion, it can be used in the blade

forming component [21].

The distribution of the stress induced by the dynamic force and pressure distribution and thermal load from the rotating blade in a 15000 rev/min that has been applied to the blade according to the von Mises criterion has been presented with various alloys in Table 3.

Table 3. The Equivalent stress range on the blade with different alloys

Alloys	Stress $_{min(Pa)}$	Stress $_{max(Pa)}$
CMXS-4	1270.1	6.8071E^{8}
In-738LC	1093.1	5.4755E^{8}
TMS-75	1161.2	6.121E^{8}

The results for superalloys supplement as Blade material are shown in Figs. 12-14.

As shown in Fig.12-14, the high stress appears at root near the hub section on the suction side of the blade. In general, the root zone of the blade is the most critical area in the stressed areas. The highest tension is in CMXS-4 alloy and the In-738LC alloy showed the lowest tension in the blade.

5. Conclusions

1. The heat transfer coefficient generated in the cooling passage wall at the pressure side surface is greater than the suction side surface of the turbine blade, and increasing the cooling air flow rate of blade has a direct effect on the heat transfer coefficient.

2. The use of various alloys, in particular with high thermal conductivity, will help us to expand and spread the heat generated by combustion at all surfaces of the blade.

3. The results obtained from simulation of the model, point to the existence of a thermal stress concentration, especially on the leading edge, the stagnation point and near the corners of the blade. Also the equivalent stress concentration near the roots is higher due to fact that roots are constrained.

4. The In-738LC superalloy has a more suitable heat range than other two superalloys due to its higher heat transfer coefficient and it also has less thermal and dynamic equivalent stresses.

5. The amount of Heat transfer coefficient on the leading Edge and the trailing Edge of the pressure side is generally greater than the heat transfer coefficient of other surfaces.

Nomenclature

E Modulus of elasticity (unit: MPa)

$\dot{m}$ Mass Flow (unit: kg/s)

C_x blade axial chord length

Re Reynolds number

Nu Nusselt number

k Thermal conductivity (unit: W/(m•K))

p Pressure (unit: Pa)

T temperature (unit: C)

α Surface coefficient of heat transfer (unit: W/(m^2•K))

ω Angular frequency (unit: rev/min)

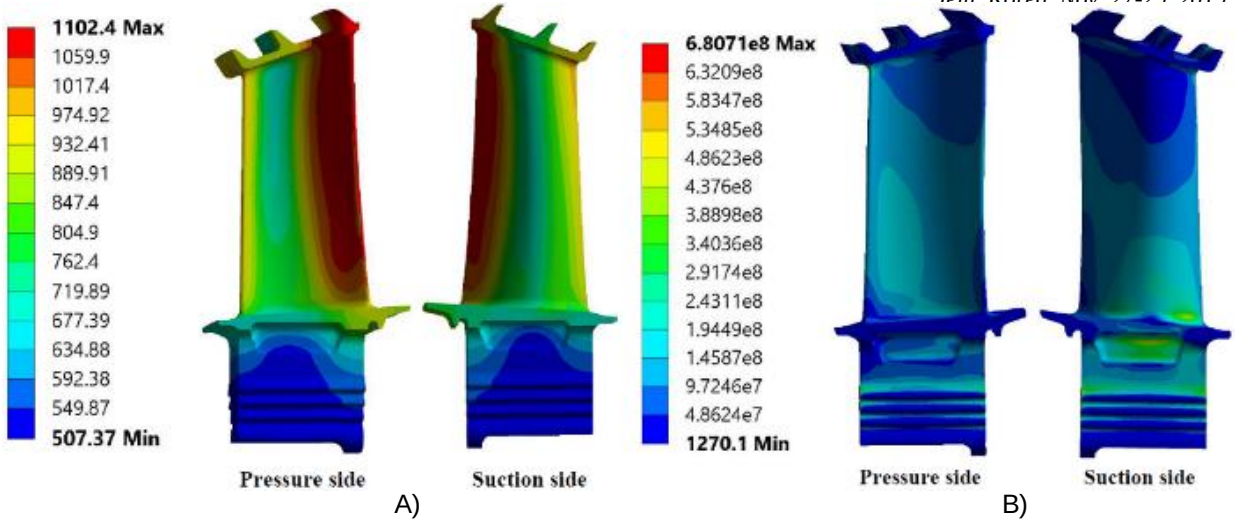

A) B)

Fig. 12. Blade with cmsx-4 material; A) Temperature (C); B) Equivalent stress (Pa)

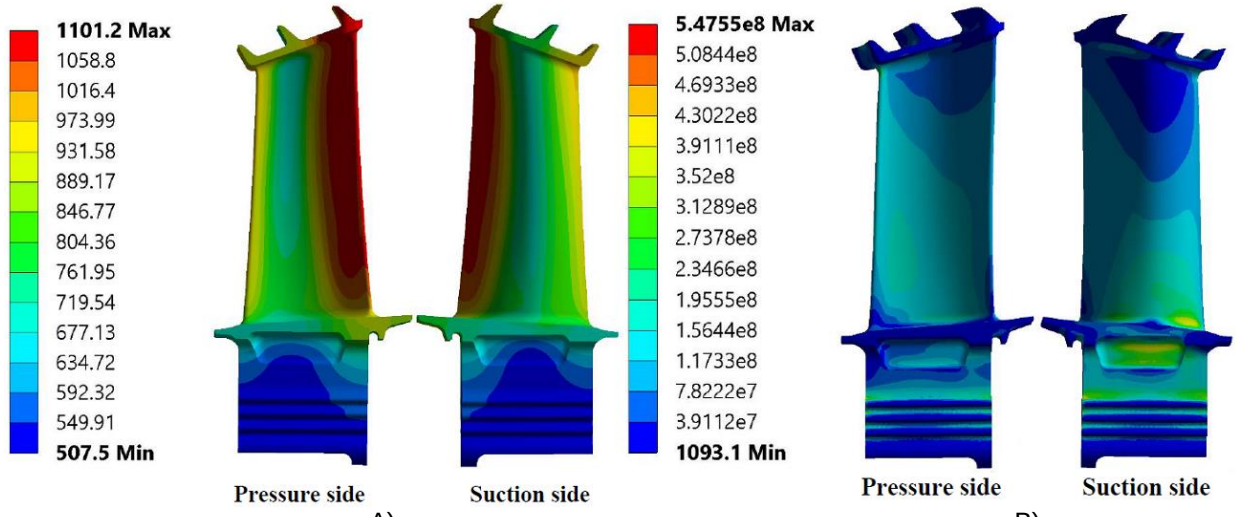

A) B)

Fig. 13. Blade with IN-738 material; A) Temperature (C); B) Equivalent stress (Pa)

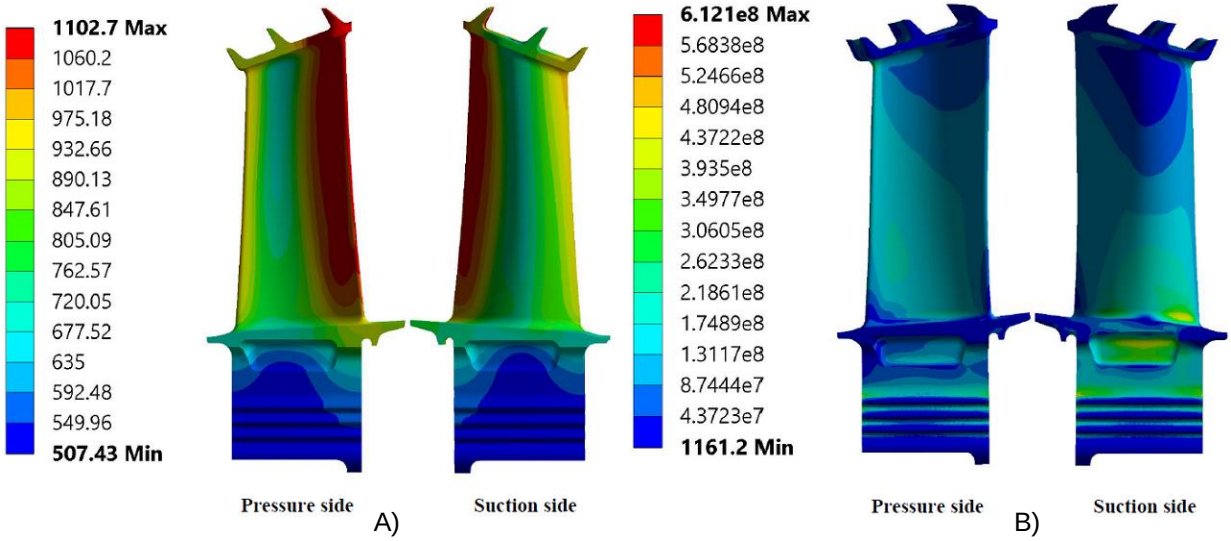

A) B)

Fig. 14. Blade with TMS-75 material; A) Temperature (C); B) Equivalent stress (Pa)

Authors' Information
Bakhshinejad Bahmbary Ailreza, born in 1995, is currently a student of Mechanical engineering at facualty of Mechanical Engineering at Shahrood University of technology, Shahrood. I received my Bsc degree from Islamic azad University of karaj, karaj, in 2017.

Competing Interests
Not applicable
Funding
Not applicable
Acknowledgements
Not applicable

References

[1] han Je, Dutta Sa, Ekkad Sr. Gas Turbine Heat Transfer and cooling Technology. 2nd ed. CRC Press Taylor & Francis Group 6000 Broken sound Parkway New York, 2013, pp. 1–7.
[2] P. Boyce M. Gas Turbine Engineering Handbook. 2nd ed. Fellow American Society of Mechanical Engineers (ASME USA) and Fellow the Institute of Diesel and Gas Turbine Engineers (IDGTE U.K.)-Gulf Profess, 2002, pp. 9-12.
[3] Sciubba E. Air-cooled gas turbine cycles e Part 1: An analytical method for the preliminary assessment of blade cooling flow rates. Energy. 2015 April1.pp. 104-114.
[4] Wróblewski W. Numerical evaluation of the blade cooling for the supercritical steam turbine. Applied Thermal Engineering. 2013, 51; 953-962.
[5] W. Zhu, J.W. Wang, L. Yang, Y.C. Zhou, Y.G. Wei, R.T. Wu. Modeling and simulation of the temperature and stress fields in a 3D turbine blade coated with thermal barrier coatings. Surface & Coatings Technology. 2017, 315; 443–453.
[6] Z.Mazur, Ramírez A, Islas J, Amezcua A. Failure analysis of a gas turbine blade made of Inconel 738LC alloy, Engineering Failure Analysis 12, 2005; 474–486.
[7] Kim Ky, Park Ju, Lee Do, Lee Ta, Cho Hy. Analysis of conjugated heat transfer. Stress and failure in a gas turbine blade with circular cooling passages. Engineering Failure Analysis 18, 2011; 1212–1222.
[8] Bolaina Ca, Teloxa Ju, Varela Ce, Sierra Fe. Thermomechanical Stress Distributions in a Gas Turbine Blade under the Effect of Cooling Flow Variations, J. Turbomach. 2013, 135(6), 9 pages.
[9] Dragomir-Stanciu Da, Oprişan Ce, Ianuş Ge, Crîşmaru Io. Study of the Influence of Ceramic Thermal Coating on the Mechanical Resistance of the Blades of Aircraft Engines. Procedia Technology 12, 2014; 329 – 333.
[10] Wang Bi, Zhang Wei, Xie Go, Xu Yin, Xiao M. Multiconfiguration Shape Optimization of Internal Cooling Systems of a Turbine Guide Vane Based on Thermomechanical and Conjugate Heat Transfer Analysis J. Heat Transfer 137(6), 2015; 8 pages.
[11] R.K Mishraa, Johny Thomasb, k.srinivasan, Vaishakhi Nandic, R.Raghavendra Bhattc. Failure analysis of an un-cooled turbine blade in an aero gas turbine engine, Engineering Failure Analysis 79, 2017; 836–844.
[12] ANSYS CFX-Solver Theory Guide, Release 14, Published in the U.S.A., November 2011.
[13] 13. J. Kurzke. Gasturb 11: Design and Off-Design Performance of Gas Turbines. 2011.
[14] P. Walsh P, Fletcher P. Gas Turbine Performance, 2nd ed. Blackwell Publishing and ASME, Fairfield, 2004.
[15] Chen-Ming Kuo. Temperature Dependent Elastic Constants of Directionally Solidified Superalloys. J. Eng. Mater. Technol. Technical Briefs. Mar 27, 2012; 134(2)
[16] Ragnhild E. Aune, Livio Battezzati,Robert Brooks, Ivan Egry, Hans-Jörg Fecht,Jean-Paul Garandet, et al. Thermophysical properties of IN738LC, MM247LC and CMSX-4 in the liquid and high temperature solid phase. TMS (The Minerals, Metals & Materials Society), Superalloys 2005; 13:467-476.
[17] D. Dye, K.T. Conlon, P.D. Lee, R.B. Rogge, R.C. Reed. Welding of single crystal superalloy CMSX-4: experiments and modeling. TMS (The Minerals, Metals & Materials Society). Superalloys 2004; 4:485-491.
[18] High-temperature, high-strength base alloy. Nicklel Development Institute; 1995 supplement.

Number 393.
[19] Robert W. Broomfield, David A. Ford, Harry K. Bhangu, Malcolm C. Thomas, Donald J. Frasier, Phil S. Burkholder, et al. Development and Turbine Engine Performance of Three Advanced Rhenium Containing Superalloys for Single Crystal and Directionally Solidified Blades and Vanes. ASME 1997 International Gas Turbine and Aeroengine Congress and Exhibition June 2–5. 1997; 4, 18 pages.
[20] Nickel Base Single Crystal Superalloy TMS-75. High Temperature Materials Group Materials Engineering Laboratory National Institute for Materials Science. July 2004.
[21] H. HARADA. High Temperature Materials for Gas Turbines:The Present and Future. Proceedings of the International Gas Turbine Congress 2003 Tokyo. November 2-7, 2003.